



ELSEVIER

Physica A 295 (2001) 507–525

PHYSICA A

www.elsevier.com/locate/physa

# Simulation of pedestrian dynamics using a two-dimensional cellular automaton

C. Burstedde\*, K. Klauck, A. Schadschneider, J. Zittartz

*Institut für Theoretische Physik, Universität zu Köln, D-50923 Köln, Germany*

Received 17 January 2001

---

## Abstract

We propose a two-dimensional cellular automaton model to simulate pedestrian traffic. It is a  $v_{\max} = 1$  model with exclusion statistics and parallel dynamics. Long-range interactions between the pedestrians are mediated by a so-called *floor field* which modifies the transition rates to neighbouring cells. This field, which can be discrete or continuous, is subject to diffusion and decay. Furthermore it can be modified by the motion of the pedestrians. Therefore, the model uses an idea similar to chemotaxis, but with pedestrians following a virtual rather than a chemical trace. Our main goal is to show that the introduction of such a floor field is sufficient to model collective effects and self-organization encountered in pedestrian dynamics, e.g. lane formation in counterflow through a large corridor. As an application we also present simulations of the evacuation of a large room with reduced visibility, e.g. due to failure of lights or smoke. © 2001 Elsevier Science B.V. All rights reserved.

*Keywords:* Cellular automata; Nonequilibrium physics; Pedestrian dynamics

---

## 1. Introduction

Considerable research has been done on the topic of traffic flow using methods from physics during the last decade [1–8]. Cellular automata inspired by the pioneering works [9–11] compose by now an important class of models. Most studies have been devoted to one-dimensional systems, where several analytic approaches exist to calculate or approximate the stationary state.

The majority of these models deals with particles which can move by more than one cell per time step (maximal velocity  $v_{\max} > 1$ ). Furthermore, it seems to be widely

---

\* Corresponding author.

*E-mail addresses:* cb@thp.uni-koeln.de (C. Burstedde), kok@thp.uni-koeln.de (K. Klauck), as@thp.uni-koeln.de (A. Schadschneider), zitt@thp.uni-koeln.de (J. Zittartz).

accepted that the most suitable update procedure is the parallel (synchronous) update. Both open and periodic boundary conditions have been considered, where problems with open boundaries are generally harder to treat analytically (for a review, see Ref. [12]).

On the other hand, pedestrian dynamics has not been studied as extensively as vehicular traffic, especially using a cellular automata approach. One reason is probably its generically two-dimensional nature. In recent years, continuum models have been most successful in modelling pedestrian dynamics. An important example are the *social force models* (see e.g. Refs. [4,8,13] and references therein). Here pedestrians are treated as particles subject to long-ranged<sup>1</sup> forces induced by the social behaviour of the individuals. This leads to (coupled) equations of motion similar to Newtonian mechanics. There are, however, important differences since e.g. in general the third law (“actio = reactio”) is not fulfilled.

In contrast to the social force models our approach is closer in spirit to the general strategy of modelling (elementary) forces on a microscopic level by the exchange of mediating particles which are bosons. It is therefore similar to *active walker models* [14,15] used so far mainly to describe trail formation, chemotaxis (see Ref. [16] for a review) etc. Here the walker leaves a trace by modifying the underground on his path. This modification is real in the sense that it could be measured in principle. For trail formation vegetation is destroyed by the walker and in chemotaxis he leaves a chemical trace. In contrast in our model the trace is virtual. Its main purpose is to transform effects of long-ranged interactions (e.g. following people walking some distance ahead) into a local interaction (with the “trace”). This allows e.g. for a much more efficient simulation on a computer.

Cellular automata for pedestrian dynamics have been proposed in Refs. [17–22]. These models can be considered as generalizations of the Biham–Middleton–Levine model for city traffic [10]. Most works have focussed on the occurrence of a jamming transition as the density of pedestrians is increased. All models have  $v_{\max} = 1$ , except for the generalization proposed in Ref. [22] which is used for analyzing evacuation processes on-board passenger ships. The other models use a kind of “sublattice-dynamics” which distinguishes between different types of pedestrians according to their preferred walking direction. Such an update is not easy to generalize to more complex situations where the walking direction can change. To our knowledge so far most other collective effects encountered empirically [4,23–26] have not been reproduced using these models. Another discrete model has been proposed earlier by Gipps and Marksjöes [27]. This model is somewhat closer in spirit to our model than the cellular automata approaches of Refs. [17–22] since the transitions are determined by the occupancies of the neighbouring cells. However, also this model cannot reproduce all the collective effects. In Ref. [28] a discretized version of the social force model has been introduced. The repulsive potentials by the pedestrians are stored in a global potential, with pedestrians reacting to the gradients of this global potential. Although this model is able to

---

<sup>1</sup> Typically decaying exponentially.

reproduce collective effects it suffers from some drawbacks [29]. It is not flexible enough to treat individual reactions to other pedestrians, and collision-avoidance is not always guaranteed for velocities greater than 1.

First we discuss some general principles we took into account in the development of our model. In contrast to vehicular traffic the time needed for acceleration and braking is negligible. The velocity distribution of pedestrians is sharply peaked [23]. These facts naturally lead to a model with  $v_{\max} = 1$  (if space is discrete), i.e., only transitions to nearest neighbours<sup>2</sup> are allowed. A greater  $v_{\max}$  would be harder to implement in 2 dimensions, especially when combined with parallel dynamics, and reduce the computational efficiency. The number of possible target cells increases quadratically with the interaction range. Furthermore one has to check whether the path is blocked by other pedestrians. This might even be ambiguous for diagonal motion and crossing trajectories.

To keep the model simple, we strongly emphasize the principle to provide the particles with as little intelligence as possible and to achieve the formation of complex structures and collective effects by means of self-organization. Effectively, there is absolutely no intelligence (i.e., look-ahead distances or multiple moves per update step depending on the distribution of occupied neighbour sites) in our model. In contrast to older approaches we do not make detailed assumptions about the human behaviour. Nevertheless, the model is able to reproduce many of the basic phenomena.

The key feature to substitute individual intelligence is the floor field. Apart from the occupation number each cell carries an additional quantity (field) which can be either discrete or continuous. This field can have its own dynamics given by diffusion and decay coefficients.

Interactions between pedestrians are repulsive for short distances. One likes to keep a minimal distance to others in order to avoid bumping into them. In the simplest version of our model this is taken into account through hard-core repulsion which prevents multiple occupation of the cells. For longer distances the interaction is often attractive. For example, when walking in a crowded area it is usually advantageous to follow directly behind the predecessor. Large crowds may also be attractive due to curiosity.

In order to produce a flow around obstacles in a simple way we also present a variant of our model where the pedestrians can be in one of two modes (or moods), “happy” or “unhappy”. These two modes are distinguished by their fluctuations. “Happy” pedestrians try to move in a preferred direction whereas “unhappy” pedestrians move in a more random fashion. This is sufficient to avoid a jamming transition due to obstacles at unrealistically low densities.

With two particle species moving in opposite directions, each with its own floor field, effects can be observed which are so far only achieved by continuous models: lane formation and oscillation of the direction of flow at doors. We consider this model

---

<sup>2</sup> Here the four diagonal neighbours are included.

to be another proof of the ability of cellular automata to create complex behaviour out of simple rules and the great applicability to all kinds of traffic flow problems.

The model can be used together with models for route selection which assign certain routes to each pedestrian. It only assumes that at every timestep for each pedestrian a transition matrix (matrix of preferences) is given.

## 2. Model

The underlying structure is a two-dimensional grid which can be closed periodically in one or both directions. Each cell can either be empty or occupied by exactly one particle (pedestrian). The size of a cell corresponds to approximately  $40 \times 40 \text{ cm}^2$ . This is the typical space occupied by a pedestrian in a dense crowd [26]. For special situations it might be desirable to use a finer discretization, e.g. such that each pedestrian occupies four cells instead of one. In this paper, however, we concentrate on the simplest case which seems to be sufficient for most purposes. The update is done in parallel for all particles. This introduces a timescale into the dynamics which can roughly be identified with the reaction time  $t_{\text{reac}}$ . In the deterministic limit, corresponding to the maximal possible walking velocity in our model, a single pedestrian (not interacting with others) moves with a velocity of one cell per timestep, i.e., 40 cm per timestep. Empirically the average velocity of a pedestrian is about 1.3 m/s [26]. This gives an estimate for the real time corresponding to one timestep in our model. Being approximately 0.3 s, it is of the order of the reaction time  $t_{\text{reac}}$ , and thus is consistent with our microscopic rules.

### 2.1. Basic rules

Each particle is given a direction of preference. From this direction, a  $3 \times 3$  *matrix of preferences* is constructed which contains the probabilities for a move of the particle. The central element describes the probability for the particle not to move at all, the remaining 8 correspond to a move to the neighbouring cells. The probabilities can be related to the velocity and the longitudinal and transversal standard deviations (see Appendix A for details). In practice, all particles of the same species share the values of these parameters and in consequence the same matrix. In the simplest case the pedestrian is allowed to move in one direction only without fluctuations and in the corresponding matrix of preference only one element is one and all others are zero (see Fig. 1).

This ansatz can easily be extended by fixing the direction of preference for each cell separately, e.g. to handle structures inside buildings. Then the particles would use the matrix belonging to the cell they occupy at a given step.

In each update step, for each particle a desired move is chosen according to these probabilities. This is done in parallel for all particles. If the target cell is occupied, the particle does not move. If it is not occupied and no other particle targets the same

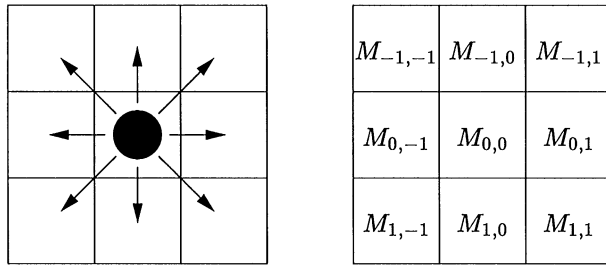


Fig. 1. A particle, its possible transitions and the associated matrix of preference  $M = (M_{ij})$ .

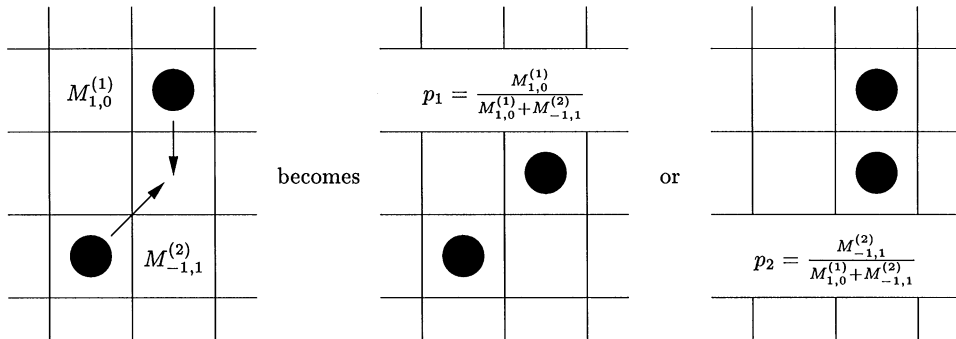


Fig. 2. Solving conflicts according to the relative probabilities for the case of two particles with matrices of preference  $M^{(1)}$  and  $M^{(2)}$ .

cell, the move is executed. If more than one particle share the same target cell, one is chosen according to the relative probabilities with which each particle chose their target. This particle moves while its rivals for the same target keep their position (see Fig. 2).

The matrix used to achieve maximum flow is clearly given by the simplest case of unidirectional fluctuation-free motion described above. Transversal fluctuations reduce the flow by introducing interference between lanes. However, this setting is not sufficient to avoid e.g. jams behind obstacles. To escape a jammed situation, the particles need a mode where they can select between different cells to move backwards or sideways in order to eventually make their way around the obstacle.

The rules presented up to here are a straightforward generalization of the CA rules used so far for the description of traffic flow [17–21]. The main difference is that in principle transitions in all directions are possible and each pedestrian  $j$  might have her own preferred direction of motion characterized by a matrix of preferences  $M^{(j)}$ . The only interaction between particles taken into account so far is hard-core exclusion.

## 2.2. Floor field

In order to reproduce certain collective phenomena it is necessary to introduce longer-ranged interactions. In some continuous models this is done using the idea of a social force [4,8,13]. Here we introduce a different approach. Since we want to keep the model as simple as possible we try to avoid using a long-range interaction explicitly. Instead we introduce the concept of a *floor field* which is modified by the pedestrians and which in turn modifies the transition probabilities. This allows to take into account interactions between pedestrians and the geometry of the system (building) in a unified and simple way without losing the advantages of local transition rules. The floor field modifies the transition probabilities in such a way that a motion into the direction of larger fields is preferred.

The floor field can be thought of as a second grid of cells underlying the grid of cells occupied by the pedestrians. It can be discrete or continuous. In this paper we will give examples for both variants. In general we distinguish between static and dynamic floor fields. The *static floor field*  $S$  does not evolve with time and is not changed by the presence of pedestrians. Such a field can be used to specify regions of space which are more attractive, e.g. an emergency exit (see the example in Section 3.1) or shop windows. This has an effect similar to a position-dependent matrix of preference but is much easier to realize.

In contrast the *dynamic floor field*  $D$  is modified by the presence of pedestrians and has its own dynamics, i.e., diffusion and decay. Usually the dynamic floor field is used to model a (“long-ranged”) attractive interaction between the pedestrians. Each pedestrian leaves a “trace”, i.e., the floor field of occupied cells is increased. Since the total transition probability is proportional to the dynamic floor field it becomes more attractive to follow in the footsteps of other pedestrians. Explicit examples where such an interaction is relevant will be given in Section 3. The dynamic floor field is also subject to diffusion and decay which leads to a dilution and finally the vanishing of the trace after some time.

In general the *transition probability*  $p_{ij}$  in direction  $(i,j)$  (see Fig. 1) is given by<sup>3</sup>

$$p_{ij} = NM_{ij}D_{ij}S_{ij}(1 - n_{ij}). \quad (1)$$

Here  $n_{ij}$  is the occupation number of the target cell in direction  $(i,j)$ , i.e.,  $n_{ij} = 0$  for an empty cell and  $n_{ij} = 1$  for an occupied cell. Therefore transitions to occupied cells are forbidden.  $N$  is a normalization factor to ensure  $\sum_{(i,j)} p_{ij} = 1$  where the sum is over the nine possible target cells. In Section 2.4.2, we will also use a slightly different form for the transition probabilities which is more general than (1).

The update rules of the full model including the interaction with the floor fields then have the following structure:

<sup>3</sup> Note that this is not a product of matrices but just the product of the corresponding matrix elements.

- (1) The dynamic floor field  $D$  is modified according to its diffusion and decay rules (see Sections 2.3 and 2.4).
- (2) For each pedestrian, the transition probabilities for a move to an unoccupied neighbour cell  $(i, j)$  is determined by the matrix of preferences and the local dynamic and static floor fields, e.g.  $p_{ij} \propto M_{ij} D_{ij} S_{ij}$ .
- (3) Each pedestrian chooses a target cell based on the probabilities of the transition matrix  $P = (p_{ij})$ .
- (4) The conflicts arising by any two or more pedestrians attempting to move to the same target cell are resolved, e.g. using the procedure described in Section 2.1.
- (5) The pedestrians which are allowed to move execute their step.
- (6) The pedestrians alter the dynamic floor field of the cell they occupied before the move.

The explicit form of the interaction between the pedestrians and the floor field and the dynamics of the floor field will be specified in Sections 2.3 and 2.4.

If more than one pedestrian species exists (i.e., two groups moving in opposite directions), each species interacts with its own floor field. In the simplest case these fields are independent from each other.

### 2.3. Discrete floor fields

In the discrete case the fields are realized through noninteracting particles which do not obey a hard-core exclusion principle. Therefore they will be called *bosons* in the following. Since the particles corresponding to the pedestrians are not allowed to share a cell these will be called *fermions*. The fermions couple to the bosons locally which drives the fermions in a preferred direction and induces a long-range interaction between the fermions.

The essence of our approach is that for each fermion the probability to jump into a direction with a larger number of bosons is increased. Thus, the motion is simply driven by gradients in the floor field, i.e., in the density of the bosons.

The first type of bosons ( $s$ -bosons) is completely static. At the beginning of a simulation for each cell  $(x, y)$  the occupation number of  $s$ -bosons  $\tau_s(x, y)$  is fixed to a specific value. Furthermore, at the beginning every cell is void of bosons of the second type, the dynamic bosons ( $d$ -bosons). Whenever a fermion jumps from site  $(x, y)$  to one of the neighbouring cells, the  $d$ -boson occupation number of cell  $(x, y)$  is increased by one (fermions leave a trace):

$$\tau_d(x, y) \rightarrow \tau_d(x, y) + 1. \quad (2)$$

After all motions of the fermions during one timestep have been performed, the oldest  $d$ -boson of each cell is destroyed with probability  $\alpha$ , if the lifetime of this boson is larger than one (i.e., it has been created during the previous update step or earlier).

Now that the two bosonic floor fields have been introduced, the update procedure for the fermions can be given. At every discrete time step  $t \rightarrow t + 1$  each fermion verifies

which of its neighbouring cells  $(i, j)$  are empty ( $n_{ij} = 0$ ). The transition probability to occupied neighbouring cells is set to zero. Thus, the probability for a jump from the centre cell  $(0, 0)$  to an unoccupied neighbour site  $(i, j)$  is given by

$$p_{ij} = N \exp(\beta J_s \Delta_s(i, j)) \exp(\beta J_d \Delta_d(i, j)) (1 - n_{ij}) d_{ij}, \quad (3)$$

where

$$\Delta_s(i, j) = \tau_s(i, j) - \tau_s(0, 0) \quad \text{and} \quad \Delta_d(i, j) = \tau_d(i, j) - \tau_d(0, 0). \quad (4)$$

$N$  is again a normalization factor to ensure  $\sum_{(i,j)} p_{ij} = 1$ .  $d_i$  is a correction factor taking into account the direction the particle in cell 0 has been coming from. The variables  $J_s$  and  $J_d$  control the coupling strength between the fermions and the  $s$ -bosons and the  $d$ -bosons, respectively.  $\beta$  plays the role of an inverse temperature. Note that the  $d$ -bosons lead to a long-range interaction between fermions in space and time.

The correction factor is introduced in order to prevent that the fermions are not confused by their own trace. One has to distinguish between three cases: If the fermion at 0 has been sitting at  $i$  at time  $t - 1$ , the  $d$ -boson sitting on top of  $i$  has been left by the fermion under consideration. Setting

$$d_{ij} = \exp(-\beta J_d), \quad (5)$$

this fermion is not taken into account in the calculation of the transition probabilities. If during the time step from  $t - 1 \rightarrow t$  the fermion has moved into the direction of the vector pointing from  $(0, 0) \rightarrow (i, j)$ , this motion shall be enhanced

$$d_{ij} = \exp(\beta J_0). \quad (6)$$

Therefore,  $J_0$  is a parameter which can be used to tune the inertia of the fermions. In all other case  $d_{ij}$  equals one.

This prescription is not free of collisions. Therefore, if  $m$  fermions try to perform a move onto the same site, only one of these fermions is allowed to perform this move. This fermion is picked at random with probability  $1/m$ . Of course one can also use the method described in Section 2.1 for the resolution of the conflicts. For the problem studied in Section 3.1 the details of the conflict resolution turned out to play no important role and we therefore used the simpler rule.

#### 2.4. Continuous floor field

In the continuous variant each cell  $j$  of the floor field carries a continuous field value  $f_j$  between 0 and 1. The basic purpose of the floor field is again to determine the transition probabilities of the pedestrians.

In the example studied in Section 3.2 we will only use a dynamic floor field, but a generalization which includes also a static field is straightforward. Since we are interested in applications related to the flow around obstacles we introduce two kinds of states in which pedestrian can be: “happy” or “unhappy”. A pedestrian becomes “unhappy” if several consecutive desired moves could not be carried out due to conflicts.



She then changes her strategy, i.e., her matrix of preferences (see Section 2.4.2). The interaction of the pedestrians with the floor field is then as follows: “Happy” pedestrians locally increase the field, and a large field aids “unhappy” pedestrians to become “happy” again, in a sense to be specified below. This is sufficient to produce a flow around obstacles, e.g. lane formation (see Section 3.2) or oscillations of the direction of flow at doors.

Without the distinction between the two states pedestrians would have the tendency to pile up in front of obstacles. If a constant flow from behind exists it will become increasingly difficult for these pedestrians to turn around and avoid the obstacle and therefore the pile will grow. For static obstacles this effect is related to the fact that our pedestrians have minimal intelligence. This assumption should be well justified in situations where they move in unknown territory and at a reduced visibility, e.g. due to smoke or failing lights. In normal situations the pedestrians can see a static obstacle (e.g. a wall) from some distance and will try to avoid them early. This can easily be incorporated in our model using a static floor field which becomes smaller just in front of the obstacle and thus reduces the corresponding transition probabilities. For dynamical obstacles, e.g. other pedestrians moving in the opposite direction, one way of avoiding unrealistic jamming properties is the introduction of different modes.

#### 2.4.1. Diffusion and decay

The dynamic floor field  $F$  is subject to diffusion and decay. It evolves according to

$$\frac{\partial F}{\partial t} = D\Delta F - \delta F, \quad (7)$$

which is discretized in the standard manner. Here  $D$  is the diffusion constant and  $\delta$  the decay constant. The ranges are restricted to  $D \in [0, \frac{1}{8}]$  and  $\delta \in [0, \frac{1}{2}]$  to suppress oscillations in the floor fields and insure that the values do not leave the interval  $[0, 1]$ .

#### 2.4.2. Floor field affects the pedestrian's desire and state

As mentioned above there are different ways to model the interaction of the floor fields with the pedestrians. Here we present a preliminary solution for the situation of pedestrians with minimal intelligence which can probably be simplified further. The form of the transition rates is slightly more general than (1). Furthermore we allow the pedestrians to be in two different modes (or moods) described by different matrices of preference. The transitions between these two modes are controlled by the floor field. The rates are, however, subject to two restrictions

- A uniform floor field should not alter the matrix of preferences.
- A non-uniform floor field should be able to change a matrix element from zero to a non-zero value.

A per-element addition of the matrix of preferences and the floor field violates the first principle, while a multiplication by e.g. Boltzmann factors violates the second.

Therefore, we are working with a compromise between the two by slightly generalizing Eq. (1)

$$p_{ij} = N(M_{ij} + b_2) \exp((F_{ij} - F_{avg})b_1), \quad (8)$$

where  $F$  denotes the floor field matrix,  $F_{avg}$  the floor field averaged over all nine relevant cells and  $P = (p_{ij})$  the transition matrix which has to be normalized by a normalization factor  $N$ . The parameters of this rule are  $b_1$  and  $b_2$ .

We introduce a second mode by switching to a different matrix of preferences. The mode described so far will be called *happy*, while the *unhappy* mode is realized by a different matrix of preferences which is simply characterized by greater standard deviations and a reduced velocity. This typically happens in high-density situations. The motion then becomes less directed and the larger fluctuations help to avoid clogging. Happy pedestrians which could not move to their desired target field in several consecutive timesteps (the exact number is a parameter of the model, in our simulations set to 3) enter the unhappy mode, while unhappy pedestrians become happy again after a certain number of consecutive allowed desires (4 in our simulations). The optimal values for these two parameters depend on the preferences of the given simulation (i.e., maximum flow versus flexible obstacle avoidance). Of course, this requires a minimal per-pedestrian memory consisting of two counters.

One could easily alter this definition by allowing a continuous choice of matrix by interpolating between the two states. This would correspond to introducing a continuous *spectrum of moods* instead of the discrete states “happy” and “unhappy”.

In addition to the mechanism for transitions between the modes described above, a unhappy pedestrian changes to a happy one immediately if the value of the floor field at its cell of origin is greater than a certain threshold. This leads to a smooth integration of unhappy pedestrians into a calm region of high flow.

#### 2.4.3. Pedestrians affect the floor field

After a pedestrian has completed a certain number of total allowed moves (the value of which is usually 3) in the happy mode, the value of the floor field of its originating cell is increased. This introduces a third counter residing in the per-pedestrian memory. The counter is set to zero at mode changes. The prescription to alter the floor field reads

$$F \rightarrow F + \min((1 - F)g_1, g_2). \quad (9)$$

The parameters of this rule are  $g_1 \in [0, 1]$  and  $g_2 \in [0, 1]$ . The way how pedestrians affect the floor field can certainly be altered slightly without changing the overall behaviour.

It is important to ignore this change in the field while modifying the matrix in the next update step to avoid artifacts (pedestrians moving backwards without reason).

With this extension, the jam behind a single obstacle composed by a line of several forbidden cells can be reduced significantly. The trade-off lies in an overall reduced

flow, as the unhappy pedestrians gravely disturb the previously unhindered movement of the pedestrians which pass to the sides of the obstacle. This evokes the need to find out for each pedestrian individually whether it might be necessary to switch to the happy state instantaneously, depending on the local situation. This can be achieved without the introduction of per-pedestrian intelligence (see section 2.4.2).

### 3. Simulations

In the following we describe the results of simulations of two typical situations, i.e., the evacuation of a large room [25] (e.g. in the case of a fire) and the formation of lanes in a large corridor [13]. We use different variants of the basic model in order to elucidate the potential of the different approaches.

#### 3.1. Evacuation of a large room

For simplicity, in the case of discrete floor fields pedestrians are only allowed to move in north ( $N$ ), west ( $W$ ), south ( $S$ ), and east ( $E$ ) direction, which leads to the following form of the matrix of preferences:

$$M = \begin{pmatrix} 0 & M_N & 0 \\ M_W & M_0 & M_E \\ 0 & M_S & 0 \end{pmatrix} \quad (10)$$

This choice means no severe restriction since transitions into the diagonal directions can be implemented quite easily.

In our simulations we have investigated the behaviour of people leaving a quadratic room with one door only. The  $s$ -bosonic field has been chosen such that the occupation number of  $s$ -bosons decreases radially from a maximum value at the door to zero at the corners opposite to the door. Typical stages of the dynamics are shown in Fig. 3.

As an example we have studied the influence of the lifetime of  $d$ -bosons (i.e., their decay probability  $\alpha$ ) on the evacuation time, i.e., the time it takes for all people to

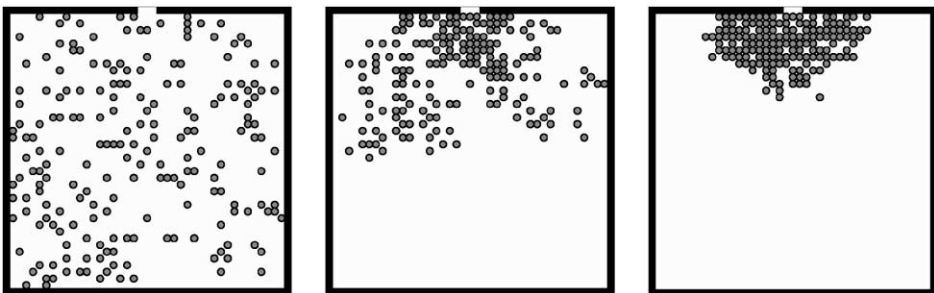


Fig. 3. People leaving a room with one door only. Displayed are three typical stages of the dynamics.

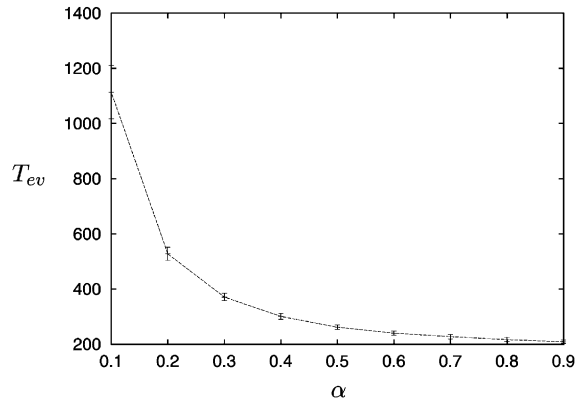


Fig. 4. Mean evacuation times  $T_{ev}$  as function of the decay probability  $\alpha$  of the  $d$ -bosons. The parameters are:  $J_s = 2$ ,  $J_d = J_0 = 1$ ,  $\beta = 10$ . The errorbars display the mean standard deviation.

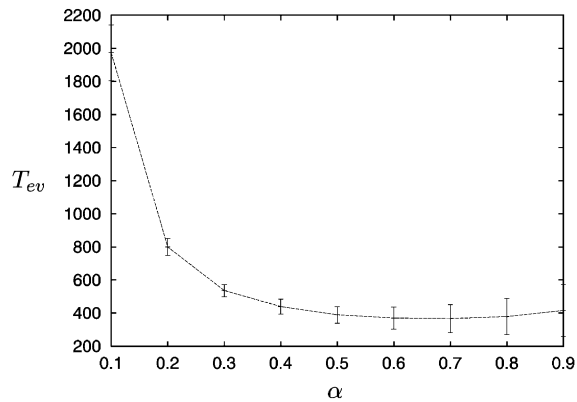


Fig. 5. Same as Fig. 4, but with  $J_s = \frac{1}{2}$ . All other parameters are the same.

leave the room. We have seen that if the coupling strength  $J_s$  to the static bosons is rather large, the evacuation time increases with an increase of the lifetime of  $d$ -bosons (see Fig. 4). Most interestingly, if  $J_s$  becomes smaller, the best evacuation times are found when the lifetime of  $d$ -bosons is fixed at some intermediate values (see Fig. 5).

This finding is very interesting, because it has the consequence that the attractive interaction of particles can lead to crucial differences in the particles' behaviour. These changes become more severe if the particles have no clear idea what the best way to the next exit is. In addition, one can see that fluctuations become much more dominant if  $J_s$  goes to zero. Therefore, in case of evacuation simulations, studying average evacuation times or—even worse—looking at one sample only might lead to wrong conclusions.

### 3.2. Lane formation in a long corridor

We present simulations of a rectangular corridor which is populated by two species of pedestrians moving in opposite directions. Parallel to the direction of motion we assume the existence of walls. Orthogonal to the direction of motion we investigated both periodic and open boundary conditions. The length of the corridor is set to 200 cells. Widths of 15 and 25 cells have been used.

With periodic boundary conditions, the density of pedestrians is fixed for each run. The program ensures that the overall number of pedestrians is evenly divided by the numbers for the different species. For open boundaries, we fix the rate at which pedestrians enter the system at the boundaries (ASEP style insertion rates). The pedestrians leave the system as soon as they reach the opposite end of the corridor.

This model clearly provides the option for a complete jam. The jamming probability with periodic boundaries at constant density increases with the length of the system. An open system can be thought of as the limit of an infinitely long periodic system, although density and entry rates do not correspond absolutely (the density in the open system is always higher than twice the insertion rate).

The update rules have the same structure as described in Section 2.2. Only step (6) is modified to

(6') The pedestrians change their mode if necessary based on their history and the floor field. They alter the (dynamic) floor field of the cell they occupied before the move.

We performed several runs for different densities and insertion rates, respectively. The focus of our attention is the parameter range where the transition from a stable flow to a complete jam takes place. The complete set of parameters for the simulations can be found in Appendix B.

Fig. 6 shows the graphical frontend running a simulation of a small periodic system. The lanes can be spotted easily, both in the main window showing the cell contents and the small windows on the right showing the floor field intensity for the two species.

To obtain information about the lanes we accumulated the pedestrian velocities at a cross section perpendicular to the direction of flow. This is done according to the formula  $j_{n+1} = j_n r + v$ , where  $j$  is the accumulated value and  $v = 0, 1$  is the velocity of the pedestrian crossing the line.  $r < 1$  is set to such a value that the characteristic number of contributing pedestrians is 100. Selected profiles are shown in Figs. 7–9. The values of the other parameters are given in the table in Appendix B. Qualitatively our results are in good agreement with those of Ref. [30] where the lane formation has been interpreted as an optimal self-organization process.

It is obvious that the lane formation in the periodic system works far better than in the open system. The floor field leads to an effective attraction of identical pedestrians while different pedestrian species separate. This results in the formation of a stable pattern in the periodic case.

In a certain density regime, these lanes are metastable. Spontaneous fluctuations can disrupt the flow in one lane causing the pedestrians to spread and interfere with other

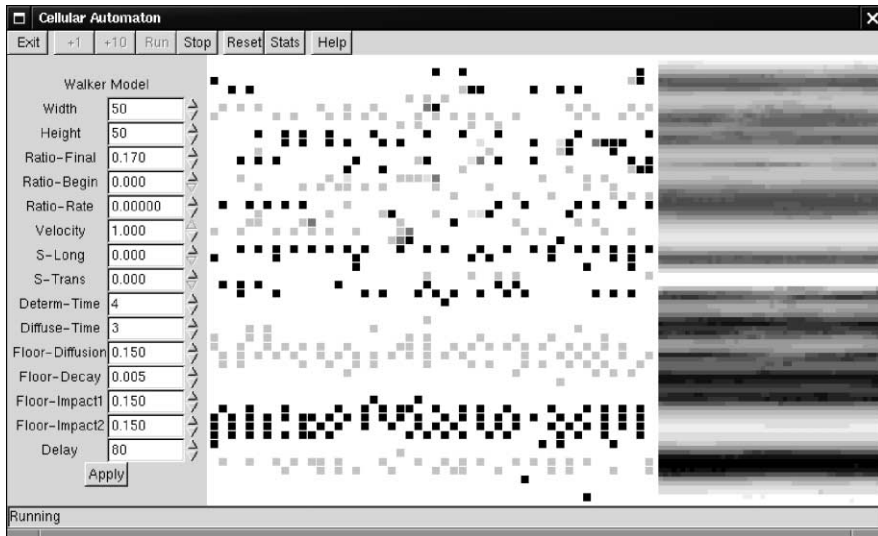


Fig. 6. Snapshot of a simulation with  $\rho = 0.17$ ,  $w = h = 50$ . The left part shows the parameter control. The central window is the corridor and the light and dark squares are right- and left-moving pedestrians, respectively. The right part shows the floor fields for the two species.

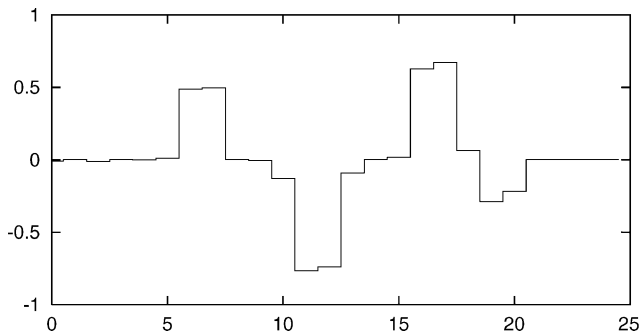


Fig. 7. Velocity profile of a periodic system with  $\rho = 0.10$ .

lanes. Eventually the system can run into a jam by this mechanism. The average time after which the system is blocked by a jam is an interesting observable which depends on the density of pedestrians. We observe large fluctuations of this observable which require many samples to find statistically significant information.

We have also found the formation of an odd number of lanes under certain conditions. This corresponds to a spontaneous breaking of the left-right symmetry of the system.

Due to the complexity of our model, the computational speed is significantly lower compared to the original models of traffic flow. A typical value measured on a SUN Sparc-10 workstation is 0.24 mega updates per second. It should still be way faster than continuous models.

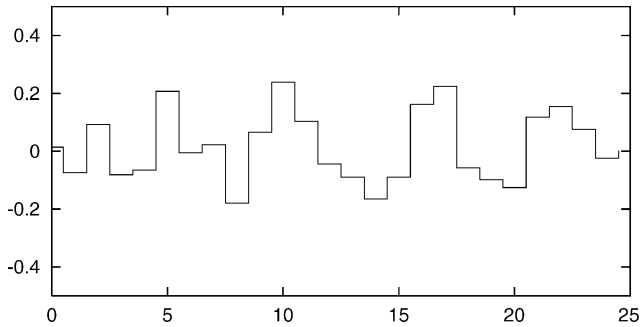


Fig. 8. Velocity profile of an open system taken at  $x = L/2$  with  $\alpha = 0.04$ .

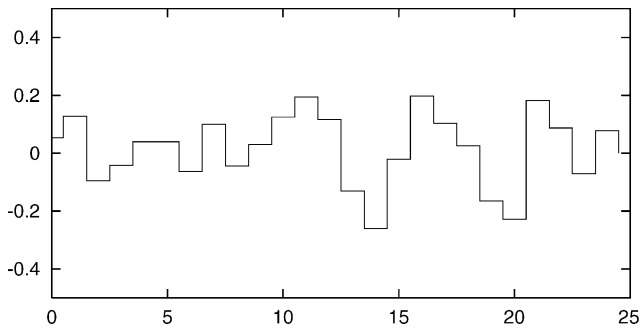


Fig. 9. Velocity profile of an open system taken at  $x = L/4$  with  $\alpha = 0.04$ .

#### 4. Conclusions

We have introduced a stochastic cellular automaton to simulate pedestrian behaviour. We focused on the general concept and the effects which can be observed with the basic approach, i.e., particle attraction and repulsion between identical and different particles respectively and lane formation.

The key mechanism is the introduction of the floor field which acts as a substitute for pedestrian intelligence and leads to collective phenomena. This floor field makes it possible to translate spatial long-ranged interactions into non-local interactions in time. The latter can be implemented much more efficiently on a computer. Another advantage is an easier treatment of complex geometries. In models with long-range interactions, e.g. the social-force models, one always has to check explicitly whether pedestrians are separated by walls in which case there should be no interaction between them. Furthermore, in these models the computational effort increases proportional to the square of the number of individuals. In contrast, in our approach it increases only linearly with the system size which is usually fixed.

The general idea in our model is similar to chemotaxis. However, the pedestrians leave a virtual trace rather than a chemical one. This virtual trace has its own dynamics

(diffusion and decay) which e.g. restricts the interaction range (in time). It is realized through a dynamical floor field which allows to give the pedestrians only minimal intelligence and to use local interactions. Together with the static floor field it offers the possibility to take different effects into account in a unified way, e.g. the social forces between the pedestrians or the geometry of the building.

We presented a rather general form of the model. Not all the features are needed in all the cases. For example for lane formation we do not need a static field. A static field might lead to a “pinning” of lanes. We have shown that our model is a good starting point for realistic applications since it is able to reproduce the basic phenomena encountered empirically. In contrast the other CA models so far have not been shown to exhibit some of the collective phenomena, e.g. lane formation etc. Other features, e.g. oscillations at doors [13], have also been observed in our simulations [32]. Quantitative results will be presented elsewhere. The model can also be applied to more complex geometries and various characteristics of a crowd can be simulated without major changes. So it should be possible to study the effects of panic (see Ref. [25] and references therein).

The description of pedestrians using a cellular automaton approach allows for very high simulation speeds. Therefore, we have the possibility to extract the complete statistical properties of our model using Monte Carlo simulations. This knowledge is of major importance if one wants to establish risk management techniques that are nowadays used for the hedging of financial assets all over the world [31].

## Acknowledgements

Part of this work has been performed within the research program of the SFB 341 (Köln–Aachen–Jülich). We like to thank H. Klüpfel, A. Keßel and D. Helbing for useful discussions.

## Appendix A. Construction of the matrix of preferences

The aim of this appendix is to show that the matrix of preferences can be directly related to observable quantities, namely the average velocities and their fluctuations. The procedure explained here to construct the matrix of preferences is not essential for the model. One could freely choose the nine matrix elements to achieve the desired behaviour of the pedestrians. However, it is not straightforward to choose five independent probabilities (one is determined by normalization and three by symmetry) in a consistent way. It is therefore convenient to look for a simpler principle, which might even simplify some calculations.

We consider first a one-dimensional setup of three adjacent fields which represents the velocities in  $I := \{-1, 0, 1\}$  from left to right. To these cells the probabilities  $p_{-1}$ ,  $p_0$  and  $p_1$  are assigned. The values of the average velocity  $v$  and of the standard



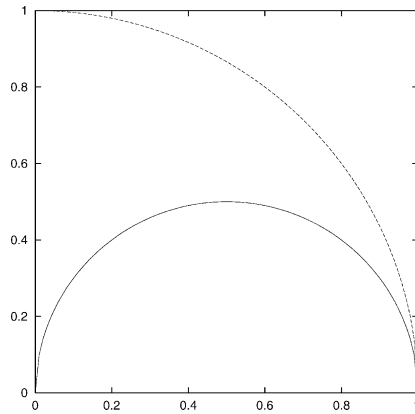


Fig. 10.  $\sigma_l$  and  $\sigma_h$  depending on  $v$ .

deviation  $\sigma$  are the parameters of this construction. This leads to three conditions which uniquely determine the probabilities

$$\sum_{i \in I} p_i = 1, \tag{A.1}$$

$$\sum_{i \in I} i p_i = v, \tag{A.2}$$

$$\sum_{i \in I} (i - v)^2 p_i = \sigma^2. \tag{A.3}$$

Not all combinations of  $v \in [-1, 1]$  and  $\sigma \in [0, 1]$  are allowed. One finds

$$p_{-1} = \frac{1}{2}(\sigma^2 + v^2 - v), \tag{A.4}$$

$$p_0 = 1 - (\sigma^2 + v^2), \tag{A.5}$$

$$p_1 = \frac{1}{2}(\sigma^2 + v^2 + v), \tag{A.6}$$

where  $\sigma$  is confined to the interval  $[\sigma_l, \sigma_h]$  with

$$\sigma_l^2 = \frac{1}{4} - (|v| - \frac{1}{2})^2 \tag{A.7}$$

$$\sigma_h^2 = 1 - v^2. \tag{A.8}$$

These restrictions are shown in Fig. 10.

To create a  $3 \times 3$  matrix  $M$ , one creates two such sets:  $\{p_{-1}, p_0, p_1\}$  with the parameters  $\{v, \sigma_v\}$  which correspond to the forward and backward movement and  $\{q_{-1}, q_0, q_1\}$  with the parameters  $\{0, \sigma_t\}$  for the (symmetric) transversal movement. These are simply multiplied

$$M_{ij} = q_i p_j, \tag{A.9}$$

Table 1

Description	Symbol	Value
Steps to happy transition		4
Steps to unhappy transition		3
Floor field diffusion	$D$	0.01875
Floor field decay	$\delta$	0.005
First active floor parameter	$b_1$	0.15
Second active floor parameter	$b_2$	0.15
First passive floor parameter	$g_1$	0.23
Second passive floor parameter	$g_2$	0.10

which produces a movement to the right for positive  $v$ . This matrix is normalized by construction. We have now achieved a reduction of free parameters from 5 to 3 and as a side effect formulated a starting point for analytical calculations.

## Appendix B. Typical parameter values

Table 1 contains the typical parameter values used in the simulations of lane formation in Section 3.2.

The first two lines show the number of consecutive allowed moves which a particle in unhappy mode needs to become happy again and the number of consecutive forbidden moves for the inverse transition, respectively.

The following two lines give the parameters for the modification of the floor field as shown in (7).

The active floor parameters determine the influence of the floor field on the particles (8), whereas the passive floor parameters describe the action of the particles on the floor field (9).

The first six of these values can be found in the lower half of the configuration panel in Fig. 6 (the diffusion constant is scaled by  $\frac{1}{8}$ ).

## References

- [1] D.E. Wolf, M. Schreckenberg, A. Bachem (Eds.), *Traffic and Granular Flow*, World Scientific, Singapore, 1996.
- [2] M. Schreckenberg, D.E. Wolf (Eds.), *Traffic and Granular Flow '97*, Springer, Berlin, 1998.
- [3] D. Helbing, H.J. Herrmann, M. Schreckenberg, D.E. Wolf (Eds.), *Traffic and Granular Flow '99: Social, Traffic, and Granular Dynamics*, Springer, Berlin, 2000.
- [4] D. Helbing, *Verkehrsdynamik: Neue Physikalische Modellierungskonzepte*, Springer, Berlin, 1997 (in German).
- [5] D. Chowdhury, L. Santen, A. Schadschneider, *Phys. Rep.* 329 (2000) 199.
- [6] A. Schadschneider, *Physica A* 285 (2000) 101.
- [7] K. Nagel, J. Esser, M. Rickert, in: D. Stauffer (Ed.), *Annual Review of Computer Physics*, Vol. 7, World Scientific, Singapore, 2000, p. 151.

- [8] D. Helbing, cond-mat/0012229.
- [9] K. Nagel, M. Schreckenberg, *J. Phys. I* 2 (1992) 2221.
- [10] O. Biham, A.A. Middleton, D. Levine, *Phys. Rev. A* 46 (1992) R6124.
- [11] M. Schreckenberg, A. Schadschneider, K. Nagel, N. Ito, *Phys. Rev. E* 51 (1995) 2939.
- [12] B. Derrida, *Phys. Rep.* 301 (1998) 65.
- [13] D. Helbing, P. Molnar, *Phys. Rev. E* 51 (1995) 4282.
- [14] D. Helbing, F. Schweitzer, J. Keltsch, P. Molnar, *Phys. Rev. E* 56 (1997) 2527.
- [15] D. Helbing, J. Keltsch, P. Molnar, *Nature* 388 (1997) 47.
- [16] E. Ben-Jacob, *Contemp. Phys.* 38 (1997) 205.
- [17] M. Fukui, Y. Ishibashi, *J. Phys. Soc. Jpn.* 68 (1999) 2861.
- [18] M. Fukui, Y. Ishibashi, *J. Phys. Soc. Jpn.* 68 (1999) 3738.
- [19] M. Muramatsu, T. Irie, T. Nagatani, *Physica A* 267 (1999) 487.
- [20] M. Muramatsu, T. Nagatani, *Physica A* 275 (2000) 281.
- [21] M. Muramatsu, T. Nagatani, *Physica A* 286 (2000) 377.
- [22] H. Klüpfel, T. Meyer-König, J. Wahle, M. Schreckenberg, in: S. Bandini, T. Worsch (Eds.), *Theory and Practical Issues on Cellular Automata*, Springer, Berlin, 2000.
- [23] L.F. Henderson, *Nature* 229 (1971) 381.
- [24] L.F. Henderson, D.J. Lyons, *Nature* 240 (1972) 353.
- [25] D. Helbing, I. Farkas, T. Vicsek, *Nature* 407 (2000) 487.
- [26] U. Weidmann, *Transporttechnik der Fussgänger*, Schriftenreihe des IVT, Vol. 80, ETH, Zürich, 1992.
- [27] P.G. Gipps, B. Marksjö, *Math. Comput. Simulation* 27 (1985) 95.
- [28] K. Bolay, Diploma Thesis, Stuttgart University, 1998; Java applets for the model can be found at <http://www.trafficforum.org/links.html>
- [29] D. Helbing, private communication.
- [30] D. Helbing, T. Vicsek, *New J. Phys.* 1 (1999) 13.1.
- [31] J.-P. Bouchaud, M. Potters, *Theory of Financial Risk*, Cambridge University Press, Cambridge, 2000.
- [32] C. Burstedde, Diploma Thesis, University of Cologne (2001); available for download at <http://www.burstedde.de/carsten/diplom.html>